	$\bar{\nu}_{ex}^{MAX}$ [cm^{-1}]	$\bar{\nu}_{em}^{MAX}$ [cm^{-1}]	W_{ex} [cm^{-1}]	W_{em} [cm^{-1}]	b_{ex}	b_{em}
RH-421	20249	15417	4185	3239	0.340	-0.025
di-4-ANEPBS	21199	16390	4176	3292	0.404	-0.226
BNBIQ	22298	17125	4327	3471	0.413	-0.219
ANNINE-5	23155	18419	3986	3427	0.492	-0.289
ANNINE-6	23673	17456	4326	3688	0.321	-0.206

Table 1. Spectral parameters of excitation and emission spectra for the S_0/S_1 transition of hemicyanine dyes in neuron membrane. The spectral maxima $\bar{\nu}_{ex}^{MAX}$ and $\bar{\nu}_{em}^{MAX}$, the spectral widths W_{ex} and W_{em} and the spectral asymmetries b_{ex} and b_{em} are obtained from twodimensional fluorescence spectra at a voltage of $V_M = -70mV$ by fitting products of two lognormal functions.

	$\Delta\bar{\nu}_{ex}^{MAX}$ [cm^{-1}]	$\Delta\bar{\nu}_{em}^{MAX}$ [cm^{-1}]	ΔW_{ex} [cm^{-1}]	ΔW_{em} [cm^{-1}]	Δb_{ex}	Δb_{em}	$\Delta F_{\bar{\nu}}^{MAX}$
RH-421	47	-18	-49	54	0.022	0.029	-0.039
di-4-ANEPBS	90	45	38	83	-0.024	0.006	-0.033
BNBIQ	103	99	8	24	-0.009	-0.014	-0.011
ANNINE-5	132	132	12	20	0.002	-0.016	-0.015
ANNINE-6	163	170	—	-19	—	0.022	0.018

Table 2. Voltage sensitivity of the spectral parameters of excitation and emission for the S_0/S_1 transition of the hemicyanine dyes in a neuron membrane. Twodimensional spectra of fluorescence are fitted with products of two lognormal functions at two different voltages. The changes of the spectral parameters - of the maxima $\Delta\bar{\nu}_{ex}^{MAX}$, $\Delta\bar{\nu}_{em}^{MAX}$, of the widths ΔW_{ex}, ΔW_{em}, of the asymmetries Δb_{ex} and Δb_{em}, and of the amplitude $\Delta F_{\bar{\nu}}^{MAX}$ - are scaled to a voltage change of $\Delta V_M = 100mV$. For ANNINE-6 the width and asymmetry of excitation was held constant because of an overlap with S_0/S_2 excitation.

	$\Delta\bar{\nu}_{ex}^{MAX}$ [cm^{-1}]			$\Delta\bar{\nu}_{em}^{MAX}$ [cm^{-1}]		
	7 param	5 param	3 param	7 param	5 param	3 param
RH-421	47	46	47	-18	-3	-6
di-4-ANEPBS	90	78	78	45	43	42
BNBIQ	103	97	96	99	91	91
ANNINE-5	132	132	134	132	123	123
ANNINE-6	163	163	163	170	159	159

Table 3. Spectral shifts of excitation and emission by a voltage change of $\Delta V_M = 100mV$. Twodimensional fluorescence spectra at two different voltages are fitted with products of two lognormal functions. The changes of the spectral maxima $\Delta\bar{\nu}_{ex}^{MAX}$ and $\Delta\bar{\nu}_{em}^{MAX}$ are shown for (i) a fit with seven changing spectral parameters (maxima, widths, spectral asymmetries, amplitude), (ii) a fit with five changing spectral parameters (maxima, widths, amplitude) and (iii) a fit with three changing spectral parameters (maxima, amplitude).

	$\bar{\nu}_{00}^{mem}$ [cm^{-1}]	$\bar{\nu}_{00}$ [cm^{-1}]	$\Delta\bar{\nu}_{00}$ [cm^{-1}]	$\Delta\bar{\nu}_{ex}^{MAX}$ [cm^{-1}]
RH-421	17833	16500	1333	47
di-4-ANEPBS	18795	16800	1995	90
BNBIQ	19712	17200	2512	103
ANNINE-5	20787	17900	2888	132
ANNINE-6	20565	17400	3165	163

Table 4. Membrane solvatochromism and electrochromism. The averages of the maxima of excitation and emission in the neuron membrane $\bar{\nu}_{00}^{mem} = \left(\bar{\nu}_{ex}^{MAX} - \bar{\nu}_{em}^{MAX}\right)/2$, the 00 energies $\bar{\nu}_{00}$ in bulk solvents, the solvatochromic blue shifts $\Delta\bar{\nu}_{00} = \bar{\nu}_{00}^{mem} - \bar{\nu}_{00}$ and the electrochromic blue shifts of excitation $\Delta\bar{\nu}_{ex}^{MAX}$ for an applied voltage change $\Delta V_M = 100mV$ in the neuron are shown. The $\bar{\nu}_{00}$ in bulk solvents are for RH-160 instead of 421 and for di-4-ANEPPS instead of di-4-ANEPBS.

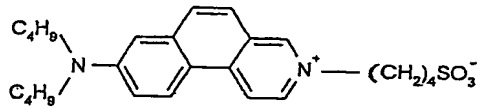

ANNINE-3

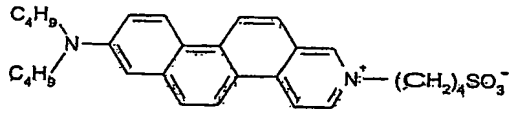

ANNINE-4

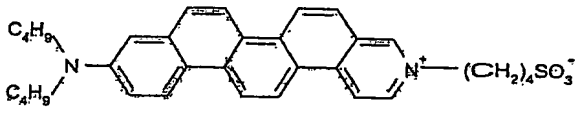

ANNINE-5

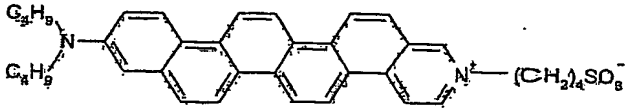

ANNINE-6

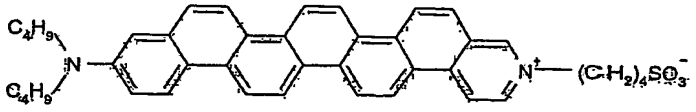

ANNINE-7

Fig. 1: Hemicyanine dyes with three to seven lineary anellated benzene rings.

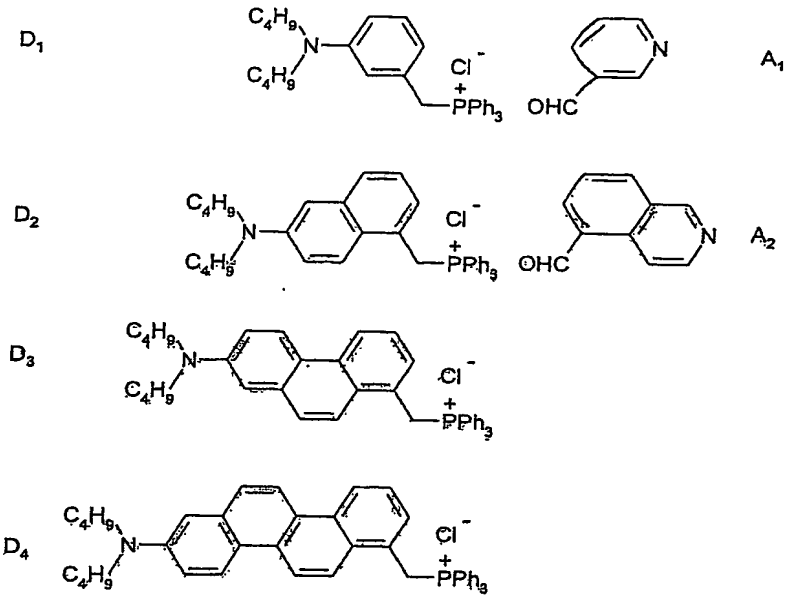

Fig. 2. Scheme of synthesis of the ANNINE dyes. The donor moieties D1 – D4 and the acceptor moieties A1 and A2 are synthetized separately. The chromphores are formed in a Wittig reaction and by subsequent ring closure in a photochemical reaction. Finally butylsulfonate groups are attached.

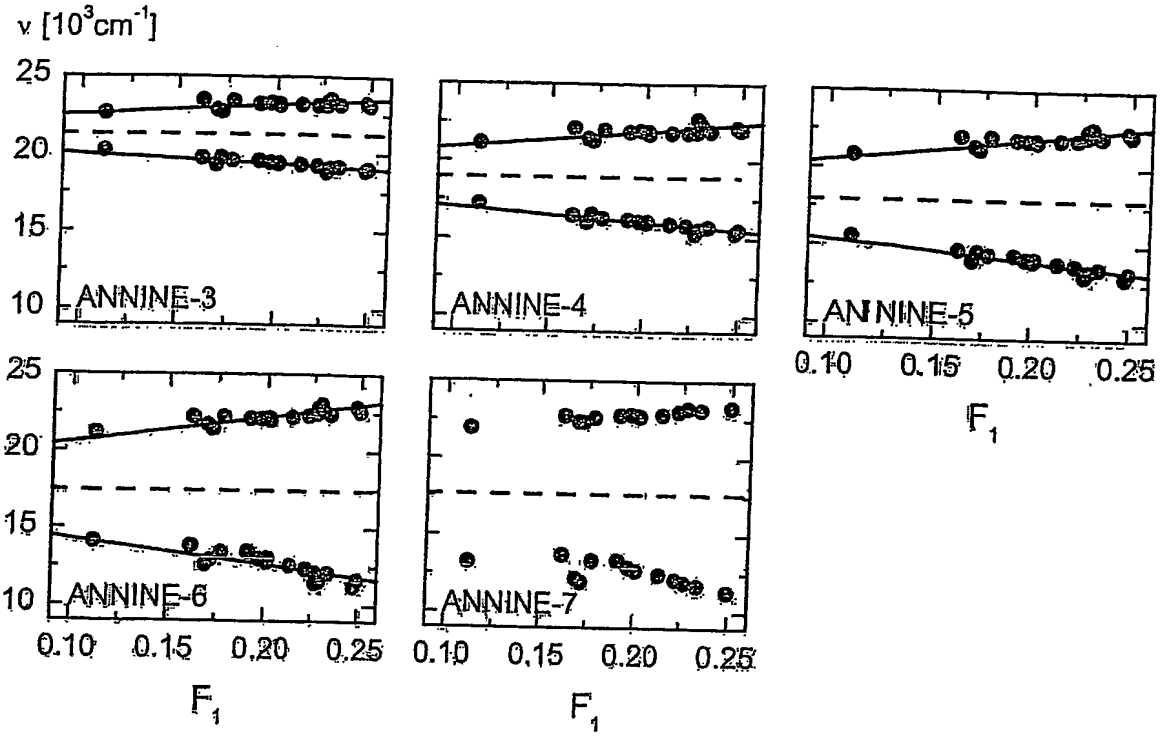

Fig. 3. Wavenumbers. Spectral data of ANNINE dyes in polar solvents. The maxima of the absorption spectra (wavenumber $\bar{\nu}_{ex}$, upper dots) and the fluorescence spectra (wavenumber $\bar{\nu}_{em}$, lower dots) are plotted versus the polarity function F_1 of 17 solvents. The straight lines are obtained from the fit of $(\bar{\nu}_{ex}+\bar{\nu}_{em})/2$ and $(\bar{\nu}_{ex}-\bar{\nu}_{em})/2$ in Fig. 4 according to a monopole-dipole model. The dashed lines are the averages of the fitted relations of excitation and emission.

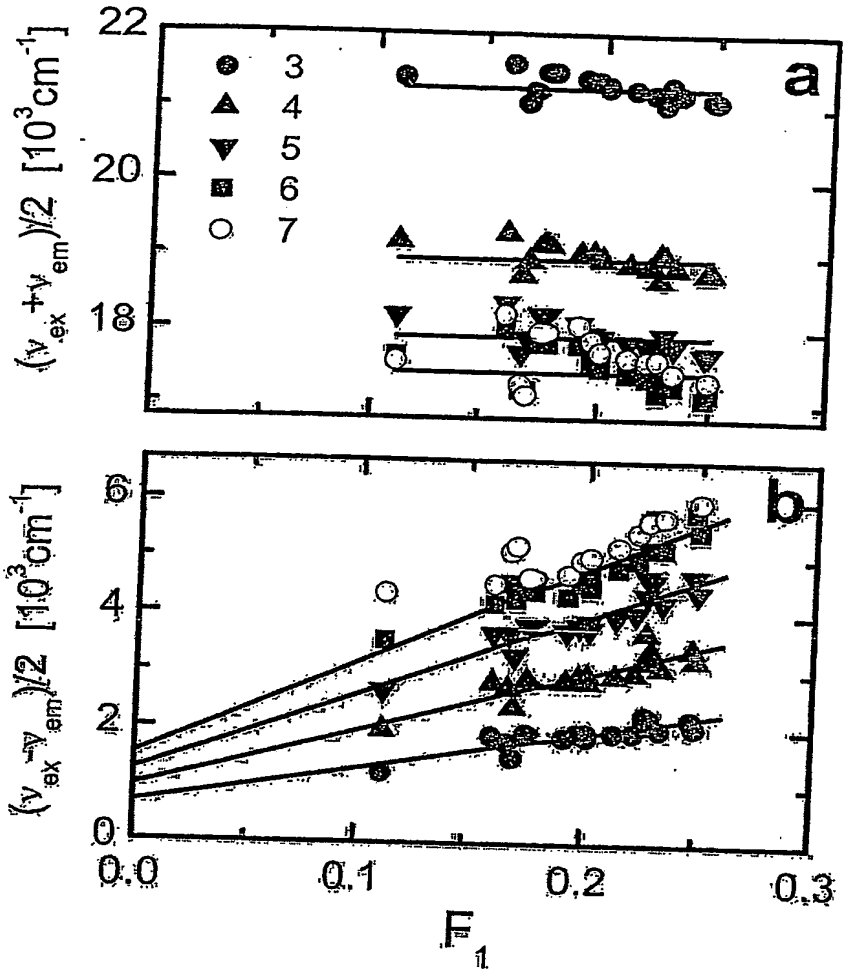

Fig. 4: Wavenumbers. Spectral features of ANNINE dyes in polar solvents. (a) Average $(\bar{\nu}_{ex}+\bar{\nu}_{em})/2$ of the spectral maxima of absorption and fluorescence versus polarity function F_1. The data are fitted with a constant wavenumber $\bar{\nu}_{00}$ for the 00 energy in vacuum. (b) Half of the Stokes shift $(\bar{\nu}_{ex}-\bar{\nu}_{em})/2$ versus polarity function F_1. The data of ANNINE-3 to ANNINE-6 are fitted with straight lines.

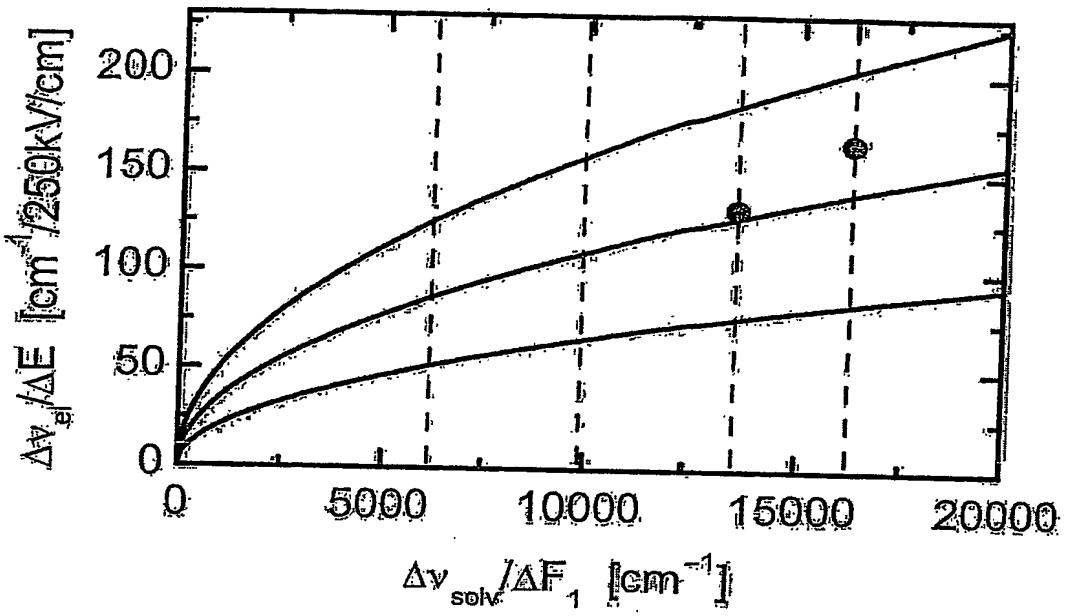

Fig. 5: Ordinate, abscissa, radius angeben. Relation of electrochromic spectral shift and solvatochromic sensitivity. The electrochromic shift $\Delta\bar{\nu}_{electro}$ expected for a voltage change of $\Delta V_M = 100mV$ across a membrane of thickness $d_M = 4nm$ is plotted versus the solvatochromic sensitivity $\Delta\bar{\nu}_{solv}$. The charge shift is assumed to be in the direction of the membrane normal with $\cos\vartheta = 1$. Three different radii of the effective radius a are considered. The experimental solvatochromic sensitivities of the ANNINE dyes are indicated by vertical lines. Two dots mark the experimental electrochromism of ANNINE-5 and ANNINE-6 in a neuron membrane.

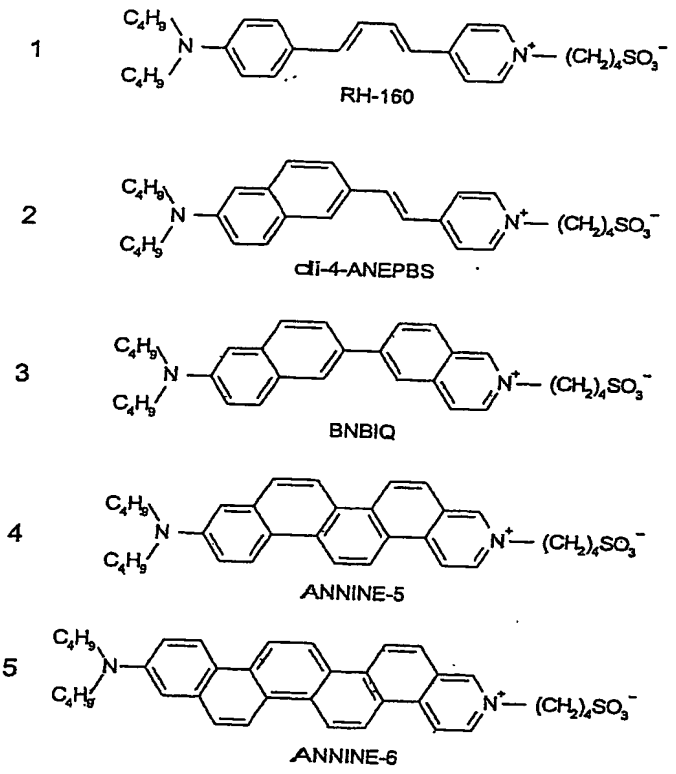

Figure 6 Voltage-sensitive amphiphilic hemicyanine dyes. (1)-(4) Homologous series with electron pushing aniline, electron pulling pyridinium and two intervening conjugated CC double bonds: styryl dye RH-160 (RH-421 with pentyl substitutents), styryl dye di-4-ANEBPS (di-4-ANEPPS with propylsulfonate), biaryl dye BNBIQ and anellated hemicyanine dye ANNINE-5. The conformation at the single bonds is matched to the structure of ANNINE-5. (5) Anellated hemicyanine dye ANNINE-6.

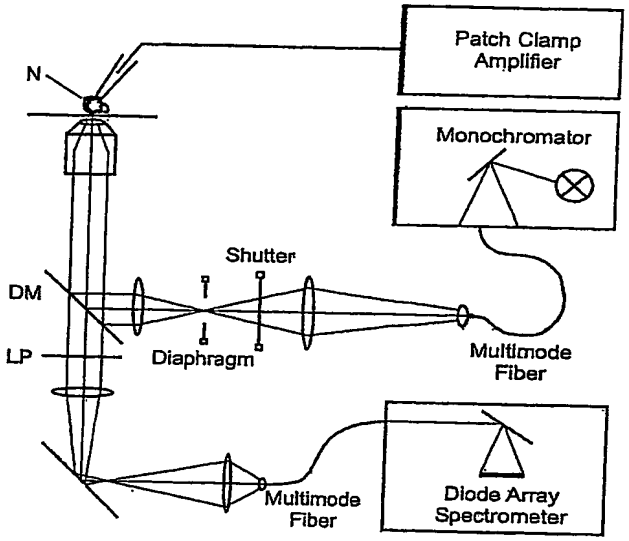

Figure 7 Experimental setup. A nerve cell (N) stained with a voltage sensitive dye is kept at a defined intracellular voltage by a micropipette using a patch-clamp amplifier. The cell is illuminated in a microscope through monochromator, shutter, dichroic mirror (DM) and objective. The fluorescence passes the dichroic mirror and a long pass filter (LP) and is detected by a diode array spectrometer. The complete fluorescence spectrum is recorded for a wide range of excitation wavelengths at two different transmembrane voltages.

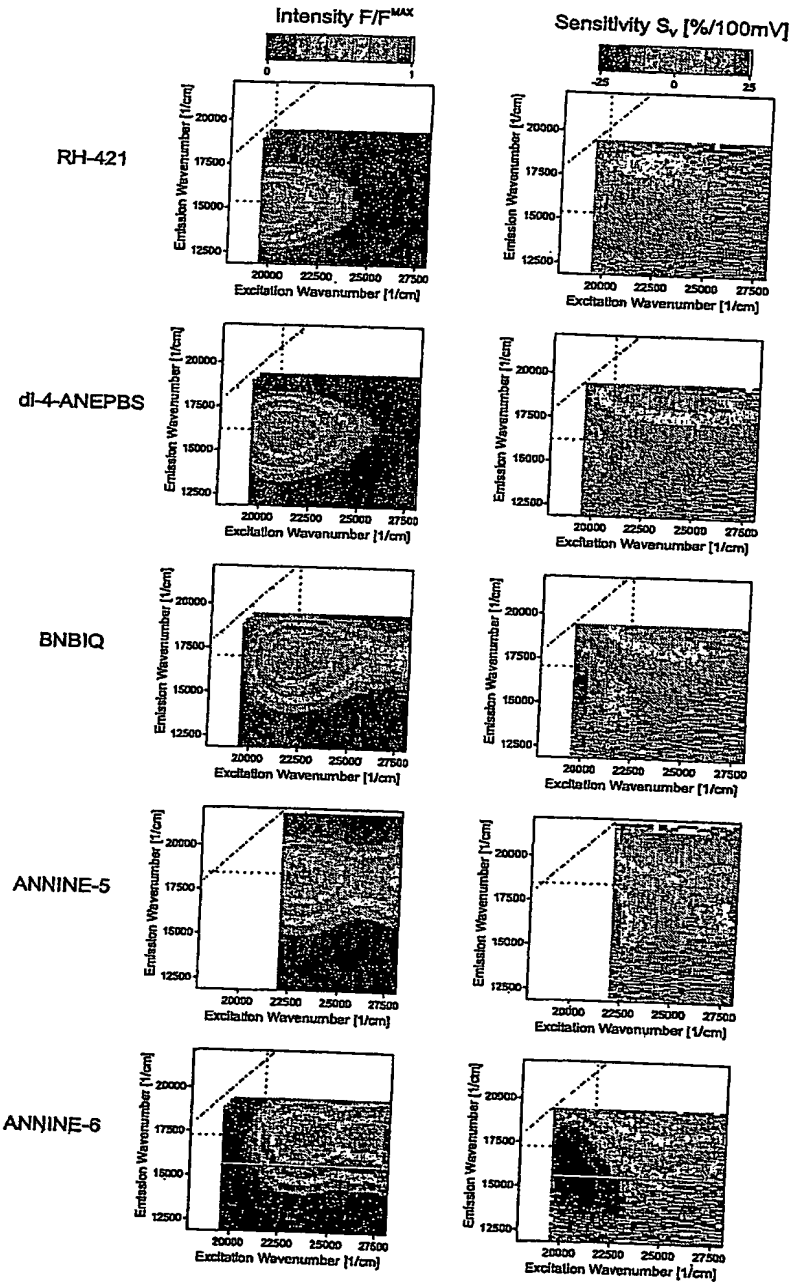

Figure 8. Experimental twodimensional fluorescence spectra. Left column: Color coded relative fluorescence intensity $F_V(\bar{\nu}_{ex},\bar{\nu}_{em})/F_V^{MAX}$ in Retzius cells at a voltage $V_M = -70mV$ as a function of the wavenumbers of excitation (abscissa) and emission (ordinate). Right column: Color coded voltage sensitivity of fluorescence $S_V(\bar{\nu}_{ex},\bar{\nu}_{em}) = \Delta F_V / F_V \Delta V_M$. The diagonal lines mark equal wavenumbers of excitation and emission. The dotted vertical and horizontal lines indicate onedimensional spectra of excitation and emission. They are chosen through the twodimensional maxima with the exception of ANNINE-6, where the excitation is chosen in the red to avoid a contribution of the S0/S2 transition.

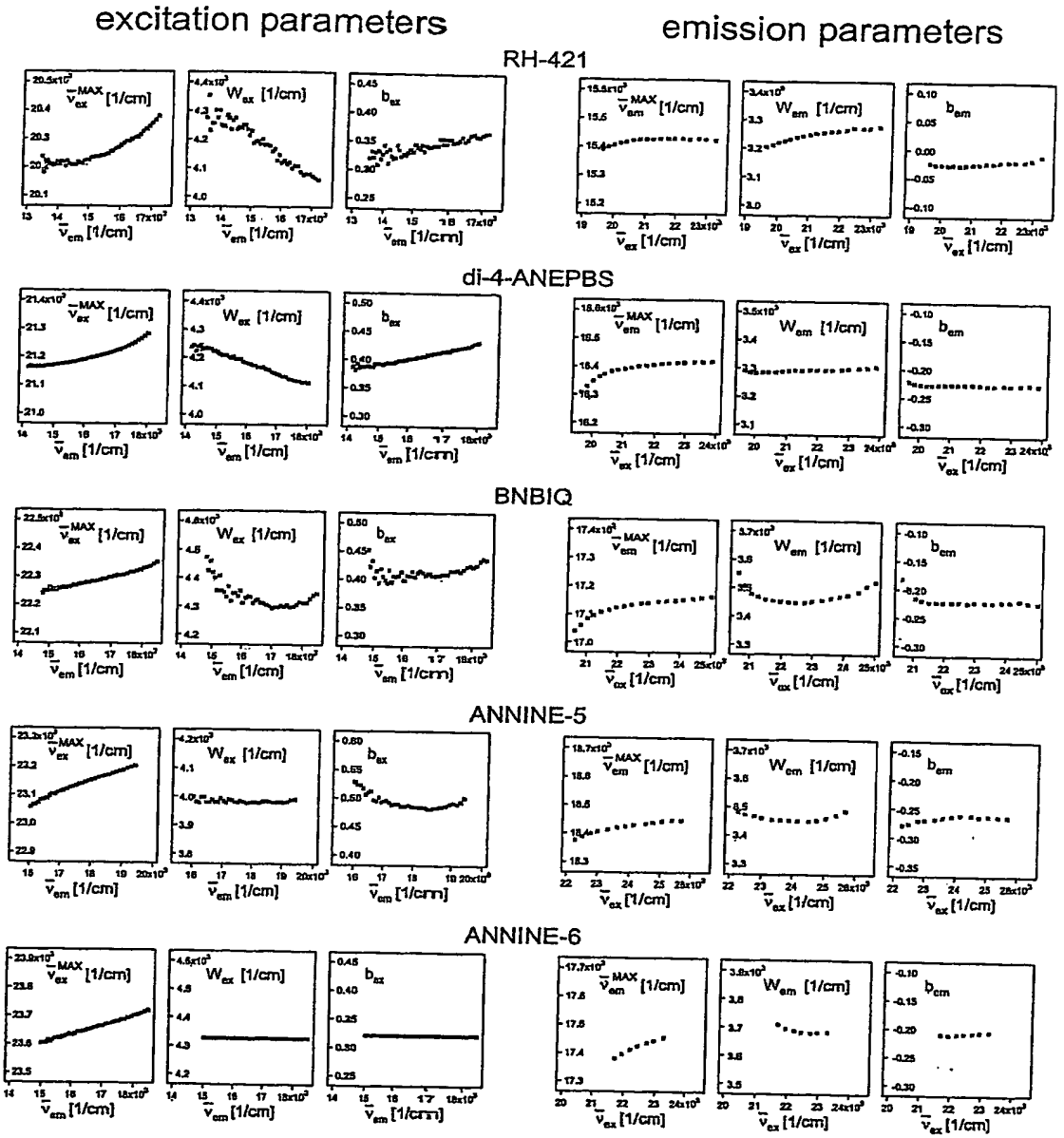

Figure 9 Mutual dependence of excitation and emission spectra. Left: Spectral parameters of the excitation spectra (maximum $\bar{\nu}_{ex}^{MAX}$, width W_{ex}, asymmetry b_{ex}) as a function of the emission wavenumber $\bar{\nu}_{em}$. Right: Spectral parameters of the emission spectra (maximum $\bar{\nu}_{em}^{MAX}$, width W_{em}, asymmetry b_{em}) as a function of the excitation wavenumber $\bar{\nu}_{ex}$.

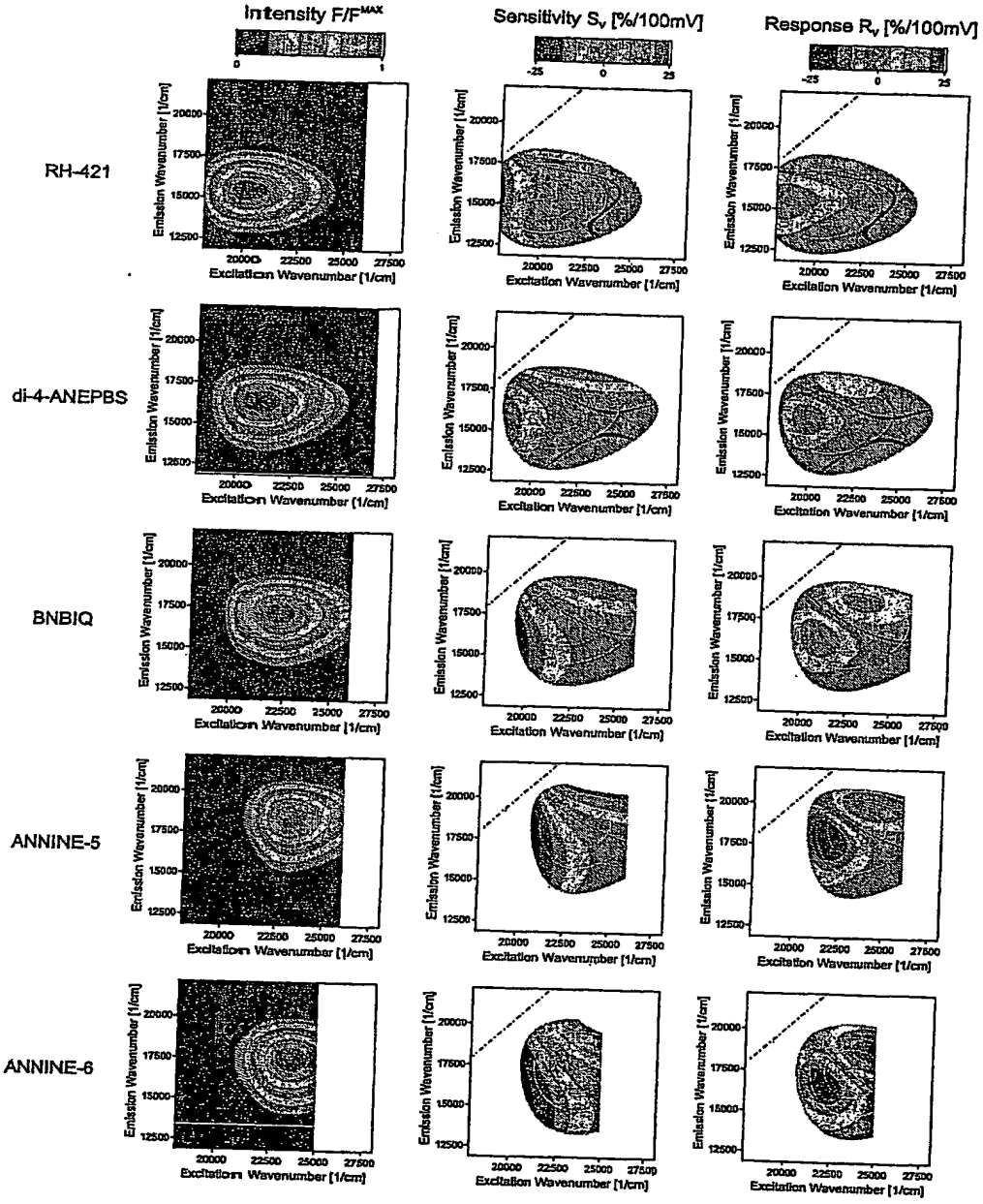

Figure 10 Twodimensional fluorescence spectra parametrized by a product of lognormal functions. Left column: color coded relative fluorescence spectra $F_{\bar{\nu}}(\bar{\nu}_{ex},\bar{\nu}_{em})/F_{\bar{\nu}}^{MAX}$ at $V_M = -70mV$. Central column: color coded sensitivity spectra $S_V(\bar{\nu}_{ex},\bar{\nu}_{em}) = \Delta F_{\bar{\nu}}/F_{\bar{\nu}}\Delta V_M$ in a range where $F_{\bar{\nu}}/F_{\bar{\nu}}^{MAX} > 0.1$ and where the S_0/S_2 transition plays a negligible role. Right column: color coded relative response spectra $R_V = \Delta F_{\bar{\nu}}/F_{\bar{\nu}}^{MAX}\Delta V_M$. The diagonals mark equal wavenumbers of excitation and emission. White lines in the sensitivity and response spectra indicate the intensity levels $F_{\bar{\nu}}/F_{\bar{\nu}}^{MAX} = 0.33$ and $F_{\bar{\nu}}/F_{\bar{\nu}}^{MAX} = 0.67$. Black lines mark the change of sign in sensitivity and response.

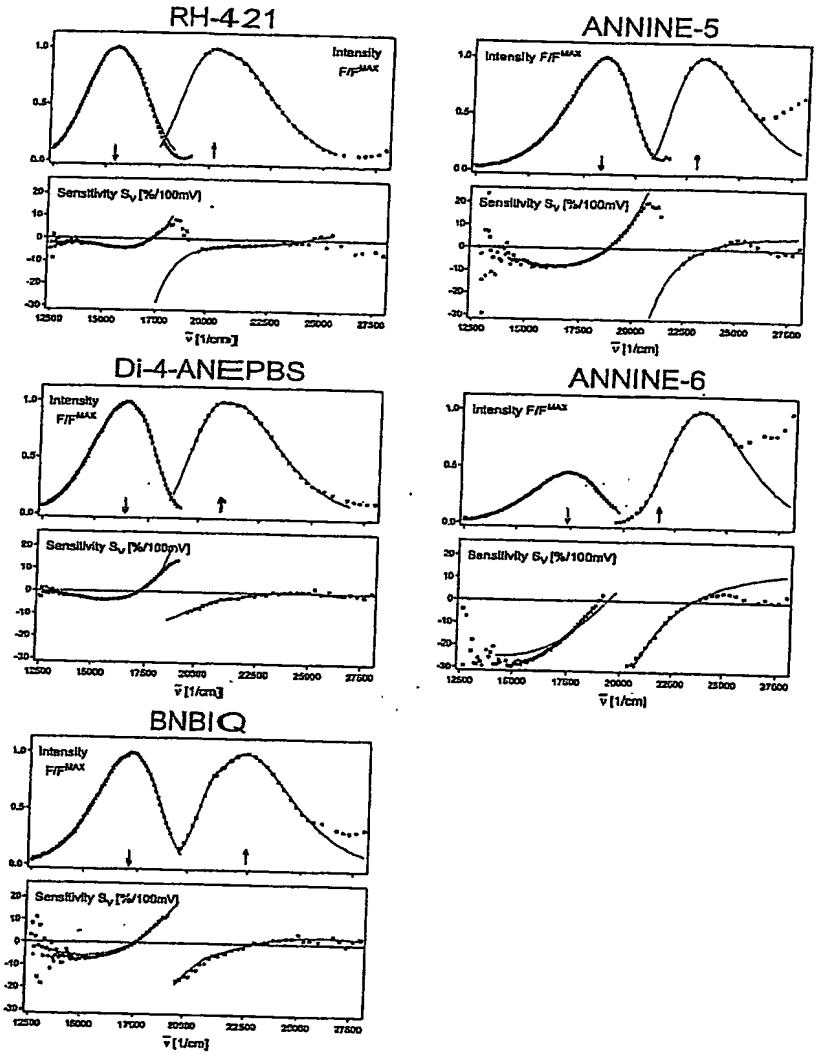

Figure 11 Onedimensional spectra of fluorescence and voltage sensitivity. Upper plots: spectra of relative intensity of emission $F_{\bar{\nu}}(\bar{\nu}_{em})/F_{\bar{\nu}}^{MAX}$ and of excitation $F_{\bar{\nu}}(\bar{\nu}_{ex})/F_{\bar{\nu}}^{MAX}$ across the twodimensional spectra as indicated in Fig. 3. Lower plots: sensitivity spectra of emission $S_{\nu}(\bar{\nu}_{em})$ and of excitation $S_{\nu}(\bar{\nu}_{ex})$. The drawn lines are onedimensional sections of the fit with a product of two lognormal functions taken from Fig. 5. The wavenumbers of excitation and emission are marked by arrows.

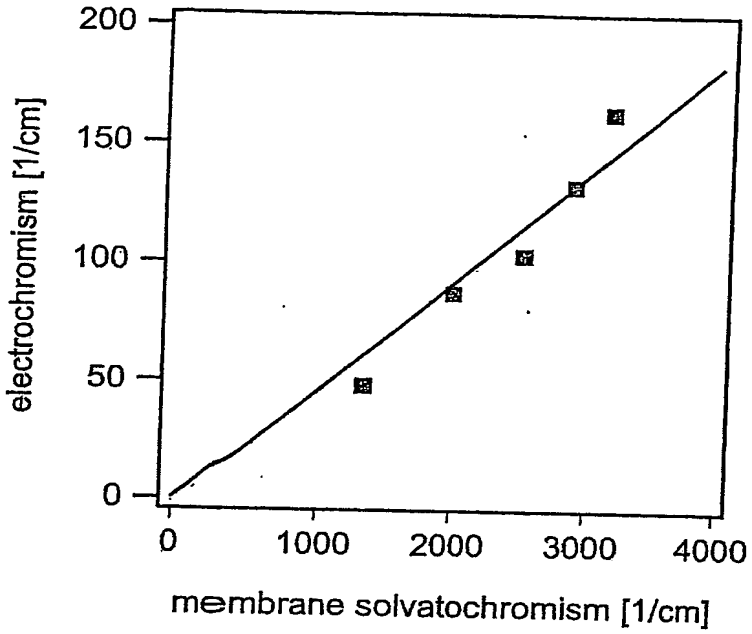

Fig.12 Electrochromism and membrane solvatochromism. Blue shift $\Delta\bar{\nu}_{ex}^{MAX}$ of the excitation spectra induced by a membrane voltage of $\Delta V_M = 100mV$ versus shift $\Delta\bar{\nu}_{00} = \bar{\nu}_{00}^{mem} - \bar{\nu}_{00}$ of the average wavenumber of excitation and emission $\bar{\nu}_{00}^{mem} = \left(\bar{\nu}_{ex}^{MAX} - \bar{\nu}_{em}^{MAX}\right)/2$ in the membrane with respect to the 00 energy $\bar{\nu}_{00}$ in bulk solvents. The dots refer to the dyes 1-5 in Fig. 1. The linear regression line has a slope of 0.045.

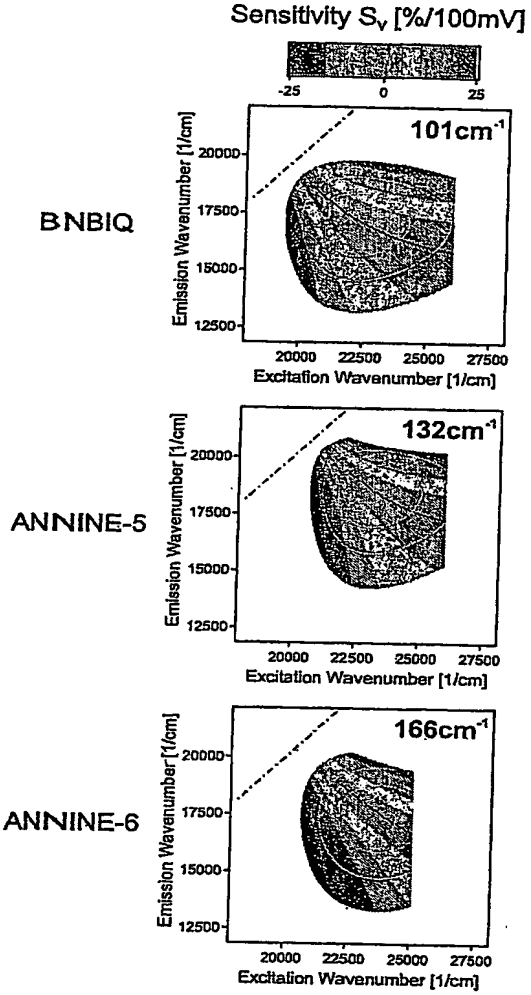

Figure 13 Voltage sensitivity for molecular Stark effect. Color coded sensitivity spectra $S_{\bar{V}}(\bar{V}_{ex},\bar{V}_{em}) = \Delta F_{\bar{V}} / F_{\bar{V}} \Delta V_M$ in a range of relative intensity $F_{\bar{V}} / F_{\bar{V}}^{MAX} > 0.1$ where the S_0/S_2 transition plays a negligible role. The spectral shifts of excitation and of emission by a voltage change of $\Delta V_M = 100mV$ are $\Delta \bar{V}_{ex,em} = 101cm^{-1}$ for BNBIQ, $\Delta \bar{V}_{ex,em} = 132cm^{-1}$ for ANNINE-5 and $\Delta \bar{V}_{ex,em} = 166cm^{-1}$ for ANNINE-6. The diagonals mark equal wavenumbers of excitation and emission. White lines in the sensitivity and response spectra indicate the intensity levels $F_{\bar{V}} / F_{\bar{V}}^{MAX} = 0.33$ and $F_{\bar{V}} / F_{\bar{V}}^{MAX} = 0.67$. Black lines mark the change of sign in sensitivity and response.

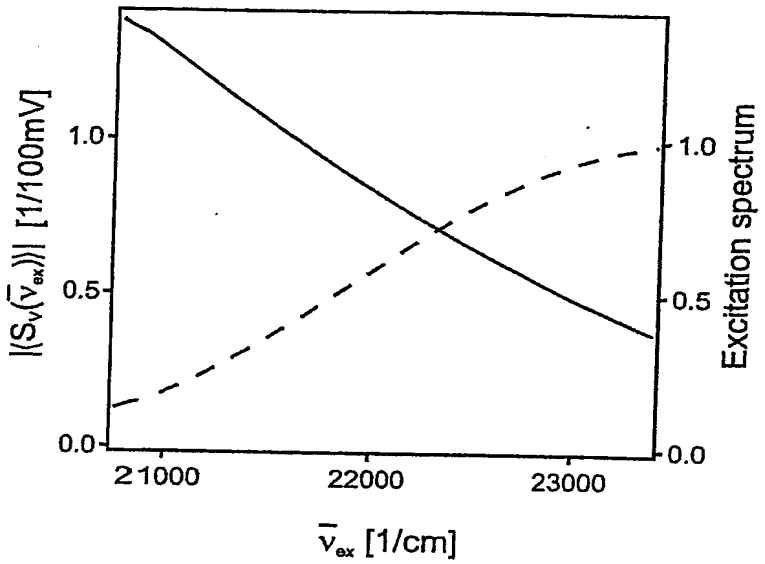

Figure 14 Weighted voltage sensitivity $\left|\left\langle S_V(\bar{\nu}_{ex})\right\rangle\right|$ of ANNINE-6 versus wavenumber of monochromatic excitation (full line) $\bar{\nu}_{ex}$. $\left|\left\langle S_V(\bar{\nu}_{ex})\right\rangle\right|$ is proportional to the signal-to-noise ratio with the constraint of a constant number of excitation processes per unit time. The detection ranges from $12000cm^{-1}$ to $17600cm^{-1}$. For comparison the relative excitation spectrum is plotted (dashed line).

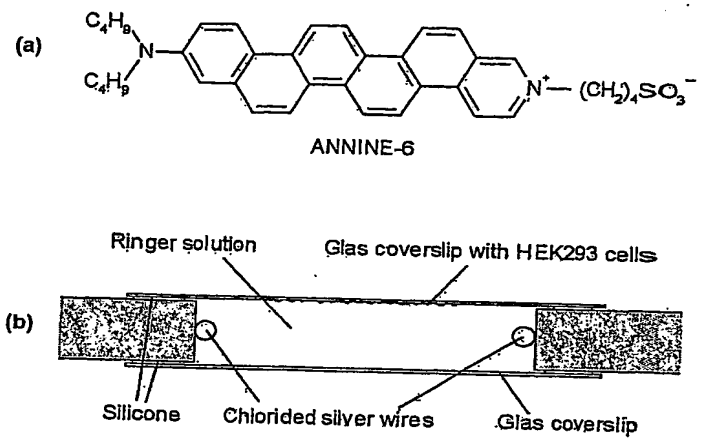

Fig.15 Structure of the new voltage-sensitive dye ANNINE-6 (a). Electric field application chamber (b). Cells are not drawn to scale. The Ringer flowes perpendicular to the paper plain.

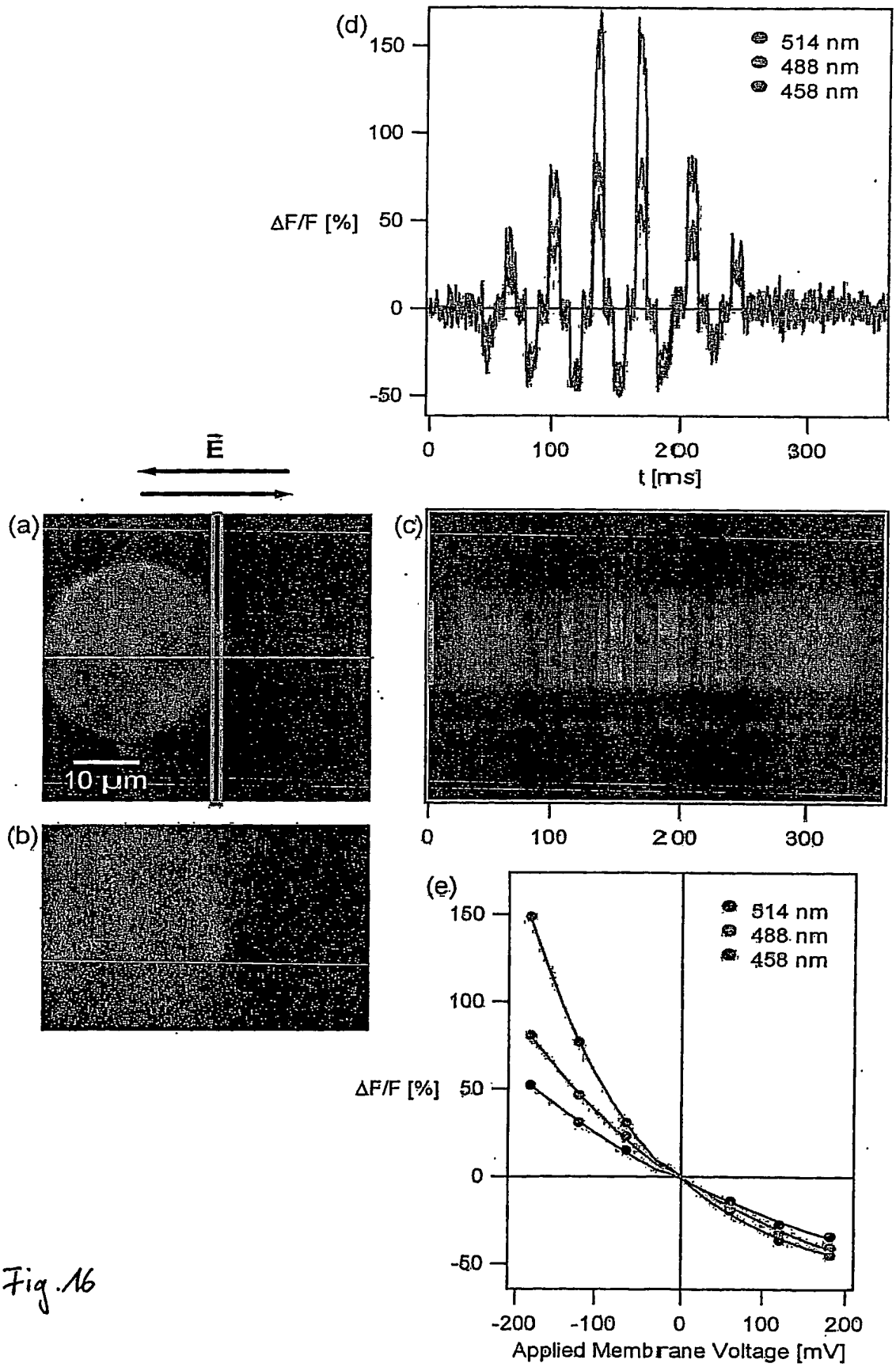
(d)
150
100
50
0
-50
ΔF/F [%]
514 nm
488 nm
458 nm
0
100
200
300
t [ms]
Ē
(a)
10 µm
(b)
(c)
0
100
200
300
(e)
150
100
50
0
-50
ΔF/F [%]
514 nm
488 nm
458 nm
-200
-100
0
100
200
Applied Membrane Voltage [mV]

Fig. 16

Fig.16 Voltage-sensitive dye signals from HEK293 cells stimulated by external electric fields. Fluorescence is excited by an Ar-ion laser. XY scan (a) and XZ scan (b) at the horizontal line marked in (a) of a cell stained with ANNINE-6 show the high membrane affinity of the amphiphilic dye. The open box in (a) markes the position of the line scan (c). Here it was scanned perpendicular to the external electric field. The line scan was aquired at an excitation wavelength of 514 *nm* and is the average of 12 measurements. The relative fluorescence changes increase when the excitation wavelength is increased from 458 *nm* over 488 *nm* to 514 *nm* (d). The 514 *nm* time trace is the average of the in (c) marked traces. The relative fluorescence changes of (d) over the applied membrane voltage is not linear but fits to an exponential curve (e). For the calculation of the applied membrane voltage only the diameter and not the shape of the cell was considered.

Figure 16a

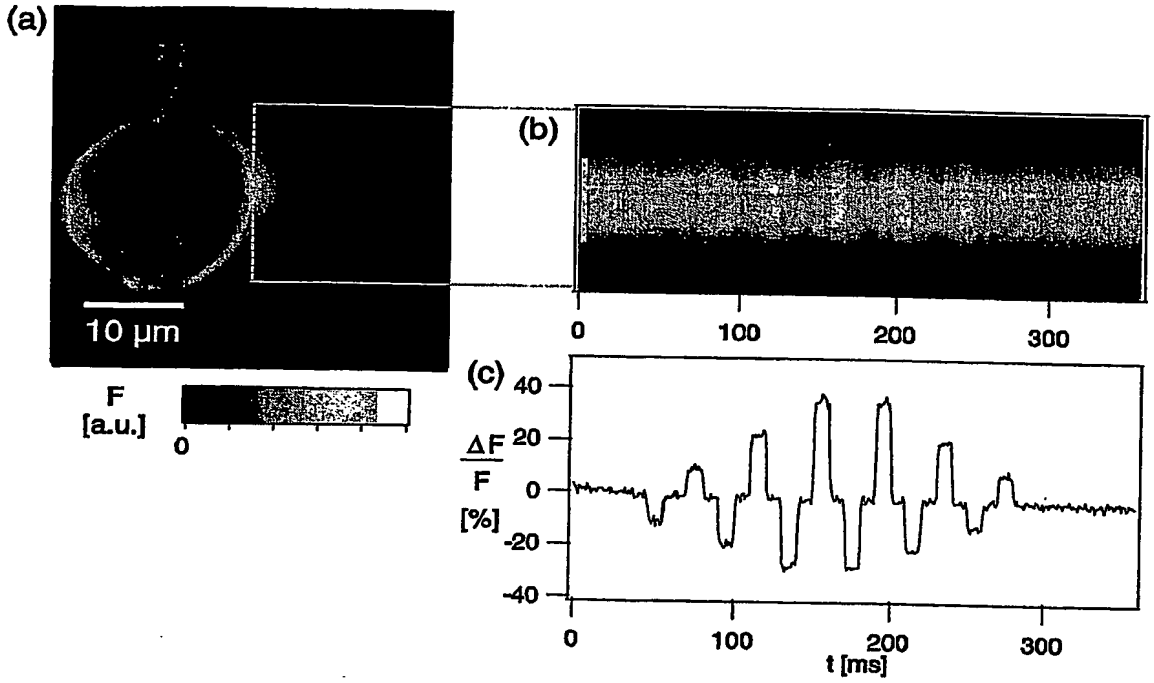

Figure 16a. Sensitivity of ANNINE-6 at an excitation wavelength of 514 nm, in a voltage-clamped HEK293 cell. (a) XY scan of the cell (note patch electrode) excited at 514 nm. The position of the line scan is marked with yellow dots. (b) Line scan of the same cell with voltage steps to +/-25 mV, +/-50 mV, and +/-75 mV. Four line scans were averaged. (c) The trace of the relative fluorescence change is the spatial average along the yellow bar in (b).

Figure 17

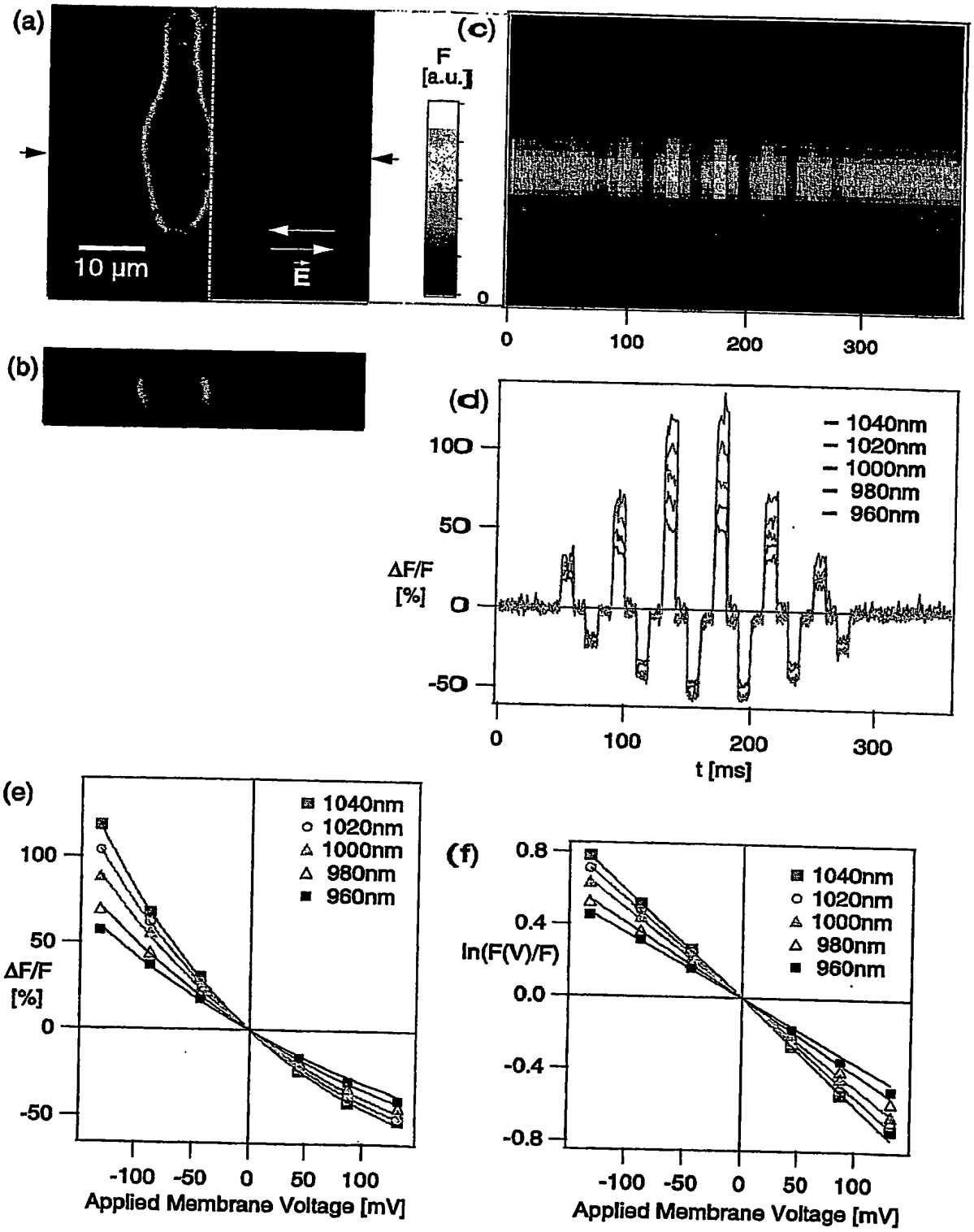

Figure 17. Signals from HEK293 cells stained with ANNINE-6, excited by 2-photon absorption and stimulated by an extracellular electric field. (a) XY scan and (b) XZ scan of a cell (excitation at 1040 nm). (c) Line scan excitation was at 1040 nm, the orientation of the

Figure 17 cont'd

electric field is given by arrows (average of 12 trials). (d) The fluorescence changes for wavelengths between 960 nm to 1040 nm. The 1040nm time trace is the spatial average of the data in (c). (e) Relative fluorescence changes *vs.* applied membrane voltage with exponential fits. (f) Same data as (e) plotted on a lin-log scale.

Figure 18

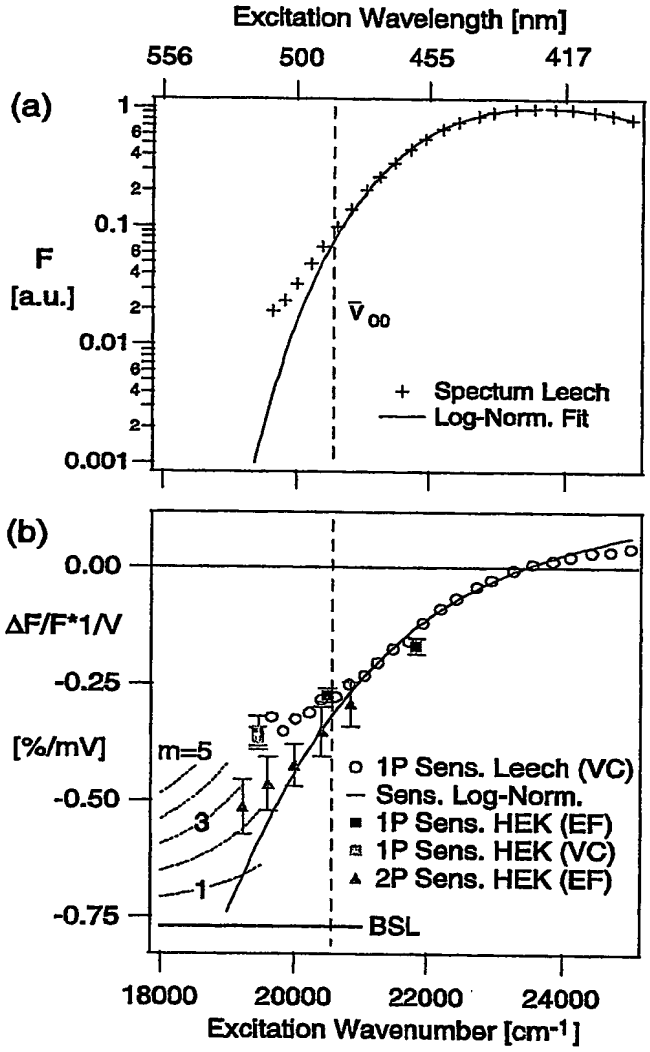

Figure 18. Excitation spectrum (a) and sensitivity (b) of ANNINE-6 near the red edge. (a) Data from a leech neuron (crosses) were fitted with a log-normal function (line) (data from Kuhn and Fromherz, 2003). (b) The sensitivity expected from the shift of the log-normal spectrum (line) and the measured leech sensitivities (open circles, data from Kuhn and Fromherz, 2003). Averaged slope sensitivities (n=4, ±standard deviation) found in HEK293 cells in our study with 1-photon excitation (blue squares: external electric field method; green square: voltage-clamp) and with 2-photon excitation (red triangles: external electric field method). For 2-photon excitation the data are plotted *vs.* the excitation energy, i.e. twice the laser wavenumber. $\bar{\nu}_{00}$ is indicated by the dashed vertical lines in (a) and (b), the Boltzmann

Figure 18 cont'd

sensitivity limit BSL for ANNINE-6 as dotted horizontal line in (b). Dotted curved lines in (b) indicate expected sensitivities using multiple vibrational modes m+1 (m=1...5).

Figure 19

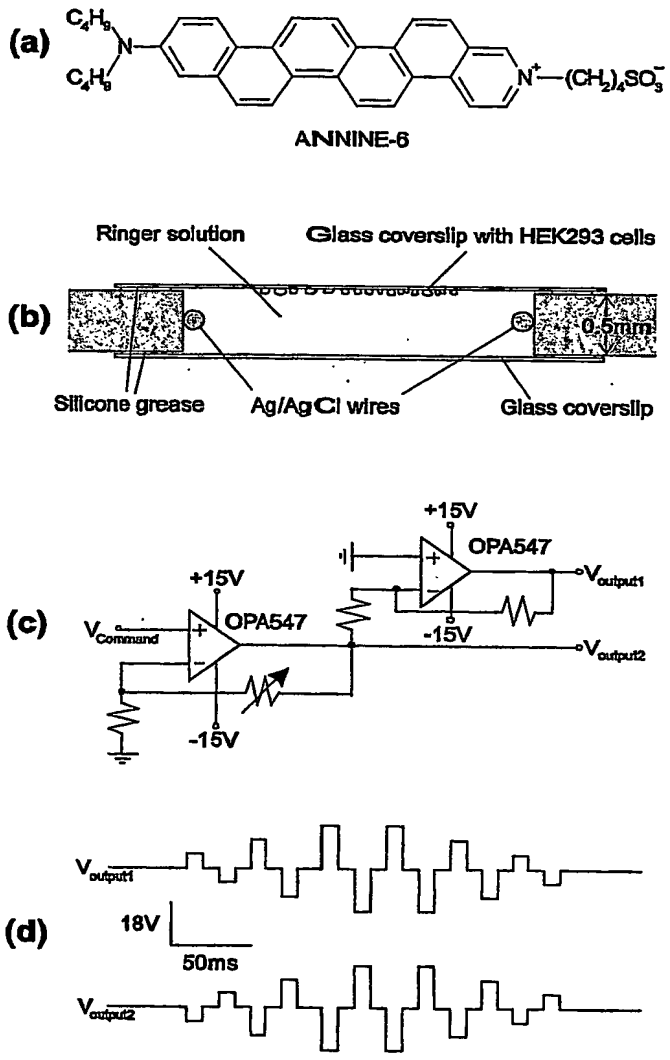

Figure 19. (a) Structure of ANNINE-6, a completely anellated hemicyanine dye; (b) cross sectional view of the electric-field application chamber. Ringer solution flows perpendicular to the paper plane. (c) Amplification circuit used to apply the electric fields. (d) Voltage pulse protocol.

Figure 20

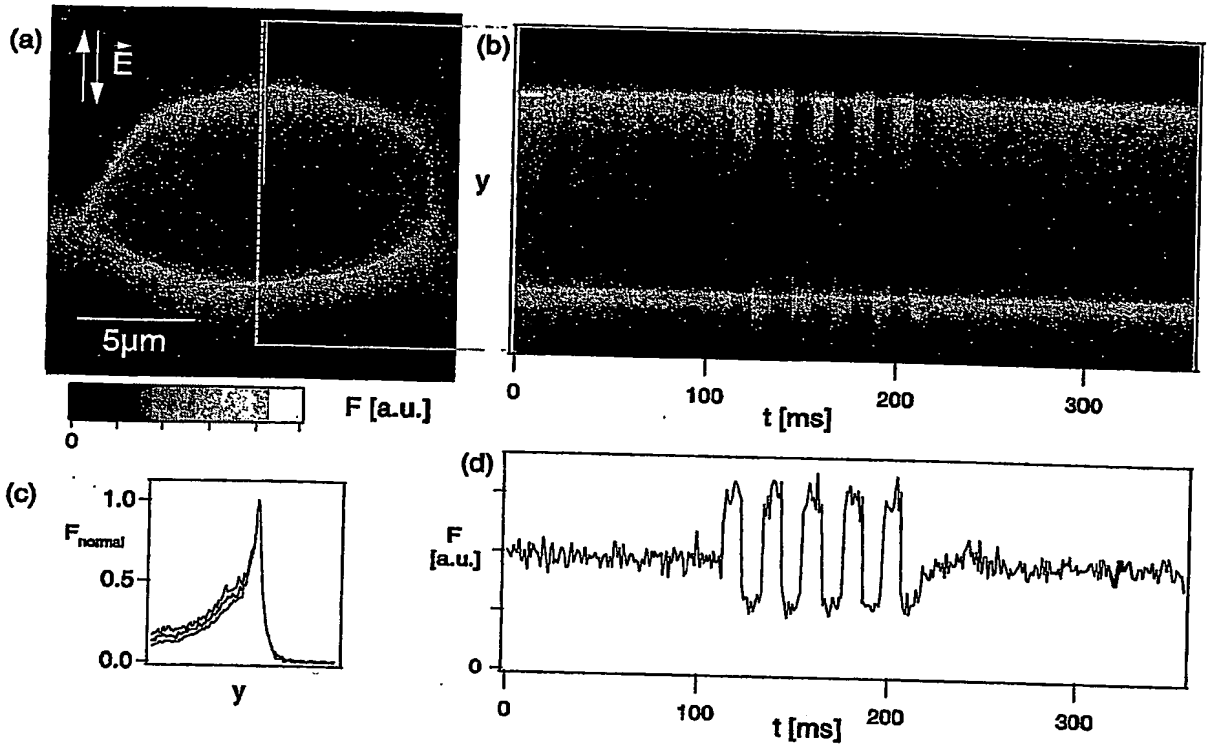

Figure 20. (a) Fluorescence of an ANNINE-6 stained HEK293 cell scanned in XY direction. A line scan was acquired at the dotted line. The lipophilic dye shows a high membrane affinity. The preferred dipole moment orientation along the membrane normal causes brighter fluorescence parallel to the laser polarization (vertical). (b) During the line scan we applied alternating external electric field pulses to show the opposing fluorescence changes on opposite cell sides. The change of membrane potential on each side was about ±110 mV. The 514 nm Ar-ion laser line was used for excitation. (c) The external electric fields cause no movement artefact: The average of 50 lines from the upper membrane in (b) (position marked in (a) by the solid yellow line) without external electric field (black line) and both external electric field directions (red and blue line) were all normalized to their intensity maximum and superimposed. (d) The average of 4 time traces marked yellow in (b) show the signal-to-noise ratio of this single trial measurement.

Figure 21

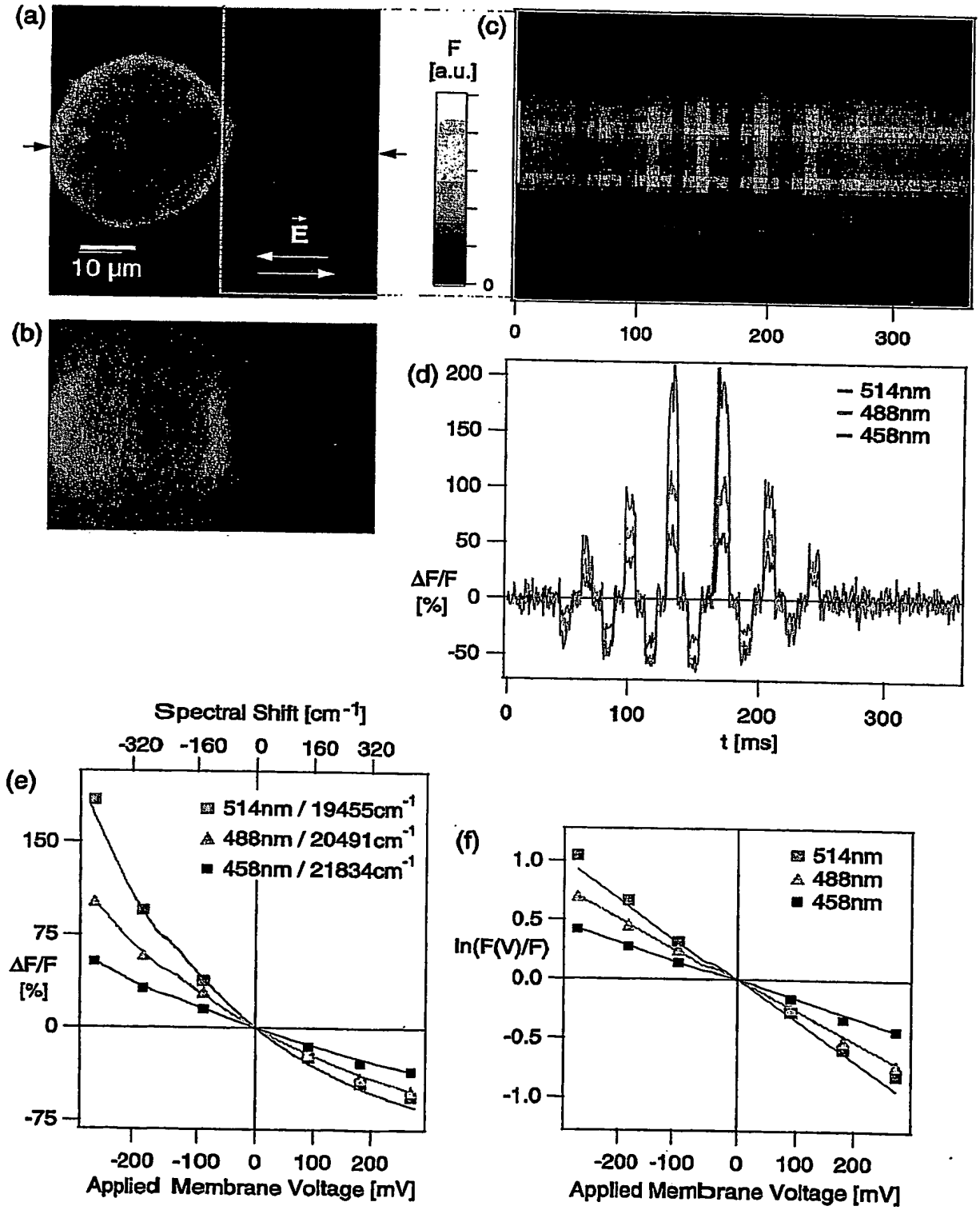

Figure 21. VSD signals in HEK293 cells stimulated by external electric fields. (a) XY fluorescence image excited at 488 nm by an Ar-ion laser. The arrows mark the position of the XZ scan shown in (b). The dotted yellow line in (a) marks the position of the line scans. The

Figure 21 cont'd

line scans were performed perpendicular to the electric field direction and along the membrane. (c) The presented line scan was acquired at an excitation wavelength of 514 nm and is the average of 12 trials. (d) The relative fluorescence changes increase when the excitation wavelength is increased from 458 nm over 488 nm to 514 nm. The time trace at 514 nm in (d) is the average of the in (c) yellow marked traces. (e) The relative fluorescence changes become more nonlinear as a function of the applied membrane voltage with increasing wavelength. For the calculation of the applied membrane voltage the diameter and a correction factor for a hemispherical cell was considered. The data points are fitted by exponential curves of the form $\left(e^{\alpha x}-1\right)$. The top scale indicates the spectral shift in wavenumbers expected from the applied membrane voltage change. (f) In a lin-log plot (fluorescence at an applied voltage over 'resting' fluorescence *vs.* membrane voltage) the data points show a quite linear relationship. The straight lines indicate $\ln\left(e^{\alpha x}\right)$.

Figure 22

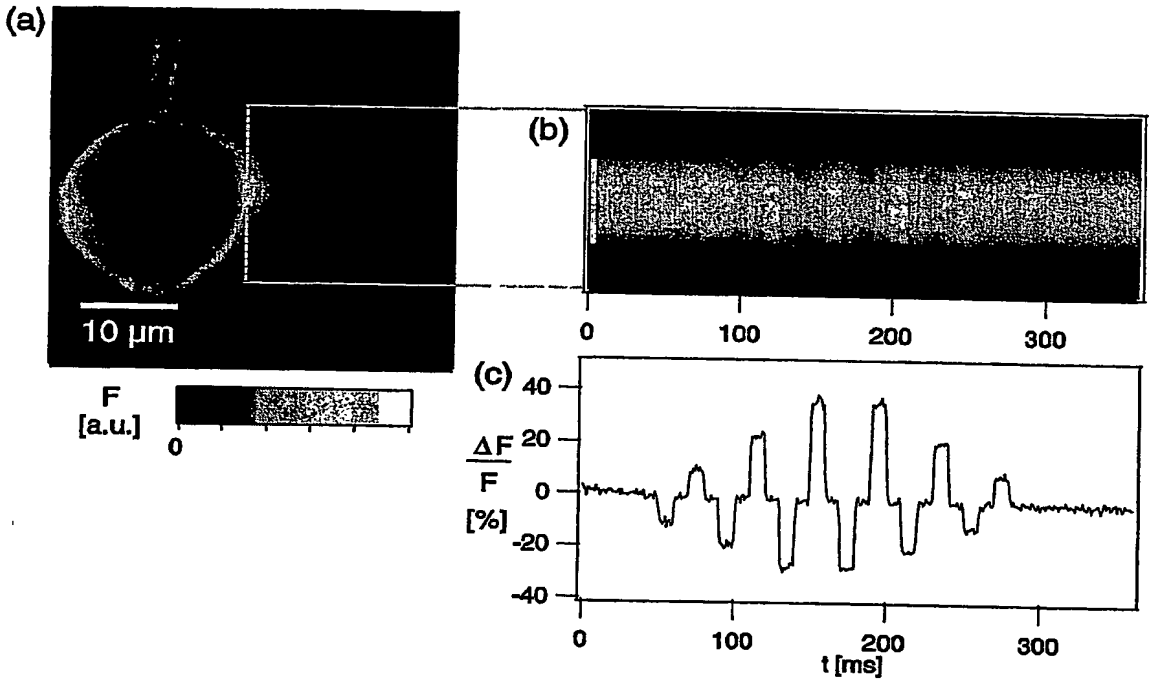

Figure 22. Sensitivity of ANNINE-6 at an excitation wavelength of 514 nm, in a voltage-clamped HEK293 cell. (a) XY scan of the cell (note patch electrode) excited at 514 nm. The position of the line scan is marked with yellow dots. (b) Line scan of the same cell with voltage steps to +/-25 mV, +/-50 mV, and +/-75 mV. Four line scans were averaged. (c) The trace of the relative fluorescence change is the spatial average along the yellow bar in (b).

Figure 23

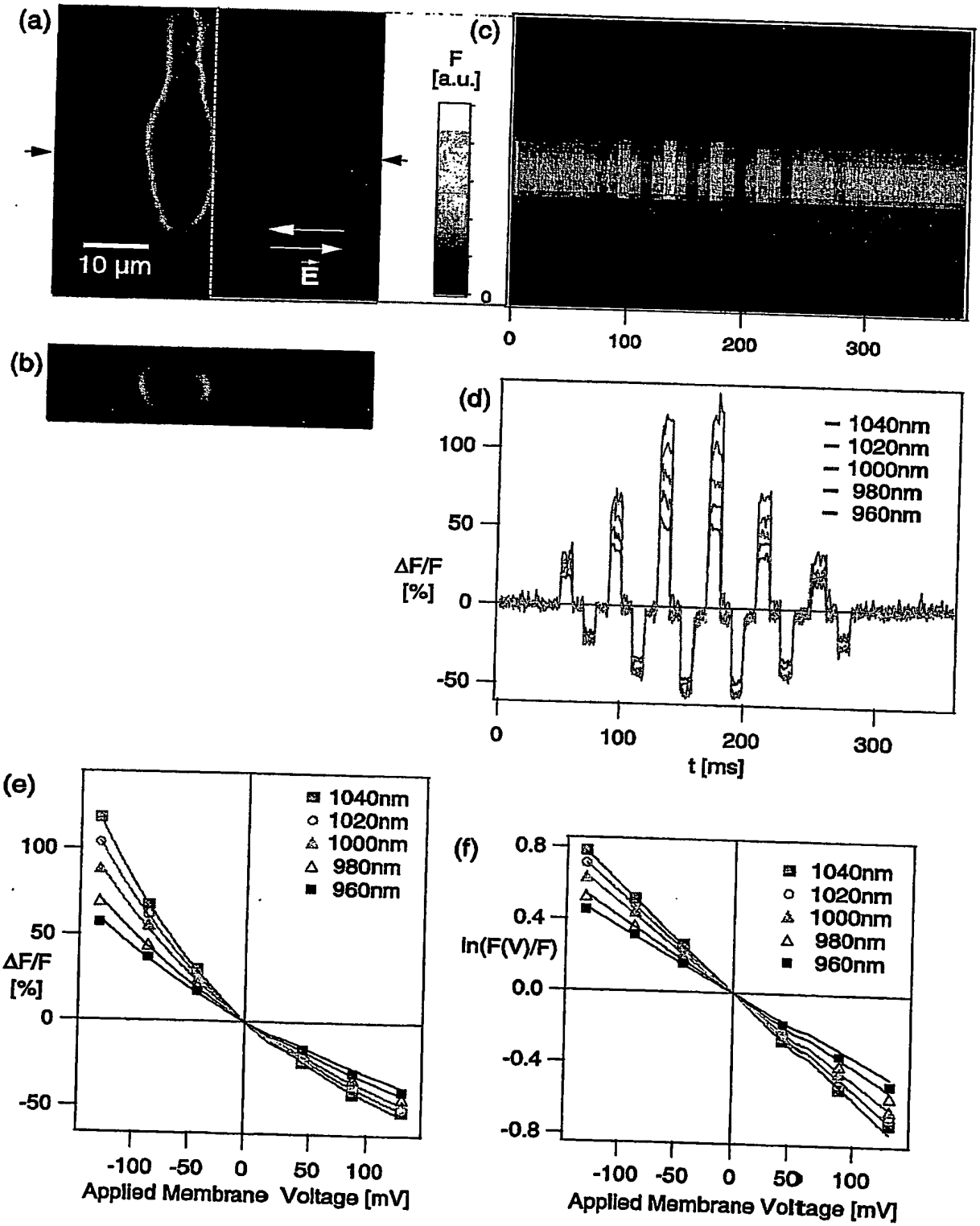

Figure 23. Signals from HEK293 cells stained with ANNINE-6, excited by 2-photon absorption and stimulated by an extracellular electric field. (a) XY scan and (b) XZ scan of a cell (excitation at 1040 nm). (c) Line scan excitation was at 1040 nm, the orientation of the

Figure 23 cont'd

electric field is given by arrows (average of 12 trials). (d) The fluorescence changes for wavelengths between 960 nm to 1040 nm. The 1040nm time trace is the spatial average of the data in (c). (e) Relative fluorescence changes *vs.* applied membrane voltage with exponential fits. (f) Same data as (e) plotted on a lin-log scale.

Figure 24

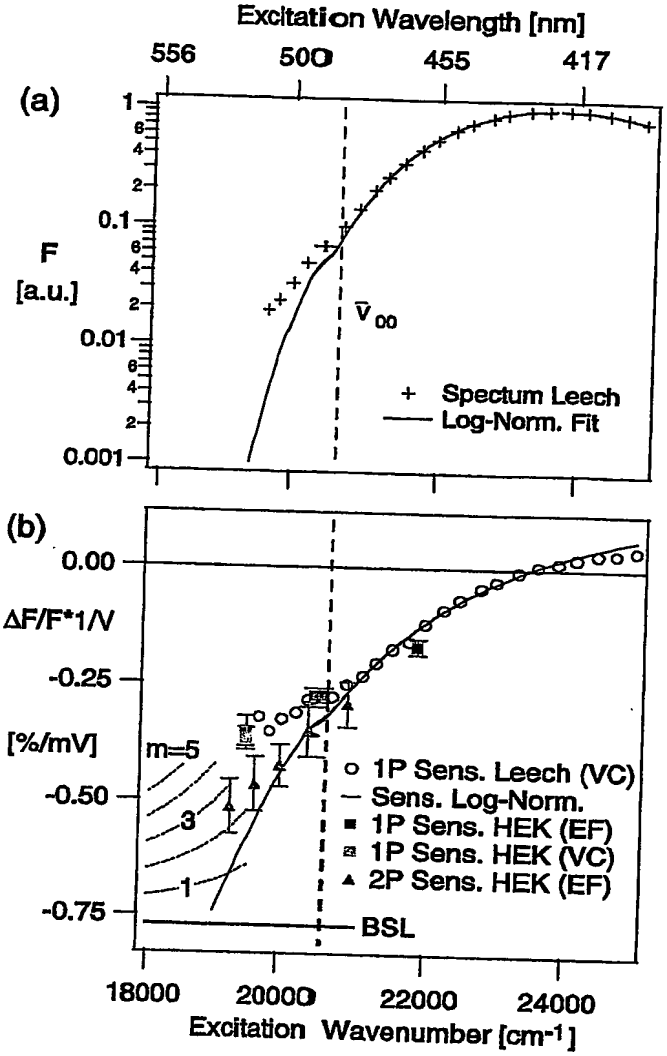

Figure 24. Excitation spectrum (a) and sensitivity (b) of ANNINE-6 near the red edge. (a) Data from a leech neuron (crosses) were fitted with a log-normal function (line) (data from Kuhn and Fromherz, 2003). (b) The sensitivity expected from the shift of the log-normal spectrum (line) and the measured leech sensitivities (open circles, data from Kuhn and Fromherz, 2003). Averaged slope sensitivities (n=4, ±standard deviation) found in HEK293 cells in our study with 1-photon excitation (blue squares: external electric field method; green square: voltage-clamp) and with 2-photon excitation (red triangles: external electric field method). For 2-photon excitation the data are plotted *vs.* the excitation energy, i.e. twice the

Figure 24 cont'd

laser wavenumber. $\bar{\nu}_{00}$ is indicated by the dashed vertical lines in (a) and (b), the Boltzmann sensitivity limit BSL for ANNTINE-6 as dotted horizontal line in (b). Dotted curved lines in (b) indicate expected sensitivities using multiple vibrational modes m+1 (m=1...5).